iScience

CellPress
OPEN ACCESS

Perspective

Breaking Free from Cobalt Reliance in Lithium-Ion Batteries

Storm William D. Gourley,[1,2] Tyler Or,[1,2] and Zhongwei Chen[1,*]

SUMMARY

The exponential growth in demand for electric vehicles (EVs) necessitates increasing supplies of low-cost and high-performance lithium-ion batteries (LIBs). Naturally, the ramp-up in LIB production raises concerns over raw material availability, where constraints can generate severe price spikes and bring the momentum and optimism of the EV market to a halt. Particularly, the reliance of cobalt in the cathode is concerning owing to its high cost, scarcity, and centralized and volatile supply chain structure. However, compositions suitable for EV applications that demonstrate high energy density and lifetime are all reliant on cobalt to some degree. In this work, we assess the necessity and feasibility of developing and commercializing cobalt-free cathode materials for LIBs. Promising cobalt-free compositions and critical areas of research are highlighted, which provide new insight into the role and contribution of cobalt.

INTRODUCTION

The global demand for lithium-ion batteries (LIBs) is no longer solely based on portable electronics but primarily driven by the electrification of the transportation industry. The increase in market share for battery and plug-in hybrid electric vehicles (EVs) over the next decade is expected to reach 20% with more than 150 million cumulative EV sales (Figure 1) (International Energy Agency, 2019). The exponential EV sales growth is driven by government incentives, such as subsidies, rebates, tax breaks, and implementation of charging stations. In addition, expanded EV driving ranges and lowered costs due to steady improvements in LIB technology are critical factors. As such, the utilization of LIBs has grown 30% per year from 2010, reaching 180 GWh in 2018 and is anticipated to reach 2,600 GWh by 2030 (World economic forum, 2019). Global expansion of LIB production capacity is projected to balloon from ~290 GWh in 2018 to ~1,700 GWh in 2028 (Figure 1) (Benchmark Mineral Intelligence, 2019). The EV-LIB market response is bidirectional—battery packs account for up to half the cost of EVs, and in order for EVs to compete with internal combustion engine (ICE) vehicles, key performance metrics must be improved including the cost-to-range ratio, safety, and power capability (Cano et al., 2018). This has galvanized efforts among research communities to develop higher-energy-density (Wh kg^{-1}) batteries at a lower cost.

COBALT SUPPLY AND DEMAND

LIB technology for consumer EVs is currently dominated by two main cathode compositions, layered $LiNi_{1-x-y}Co_xAl_yO_2$, $x + y < 0.2$ (NCA), and $LiNi_xMn_yCo_zO_2$, $x + y + z = 1$ (NMC) (Grand View Research, 2017). Owing to the degree of commercialization and production of these materials worldwide, it is expected that they will remain the primary cathode chemistries for LIBs over the next decade. However, large-scale LIB production raises concerns over resource availability. It is estimated that 50%–80% of the production cost of LIBs is associated with materials, with up to 50% of this ascribed to the cathode active material (AVICENNE Energy, 2017; Berckmans et al., 2017). As LIB manufacturing costs have substantially decreased owing to economies of scale, transitions toward larger cell formats, and maturity in battery pack production techniques, the material input cost will become more prevalent (Few et al., 2018; Nykvist and Nilsson, 2015). Constraints in the supply of raw materials can lead to severe price fluctuations and make LIBs unreasonable for large-scale applications, bringing the momentum and optimism of the EV market to a halt.

Among the raw resources required for LIB production, concerns have been raised over the supply chain of lithium and cobalt, which is closely linked with battery production. Although the exact quantity of recoverable global lithium reserves is difficult to determine, most projections concur that they are sufficient to meet long-term projected demands (up to 2100) (Gruber et al., 2011; Narins, 2017). However, there are

[1]Department of Chemical Engineering, University of Waterloo, 200 University Avenue West, Waterloo, ON N2L 3G1, Canada

[2]These authors contributed equally

*Correspondence: zhwchen@uwaterloo.ca

https://doi.org/10.1016/j.isci.2020.101505

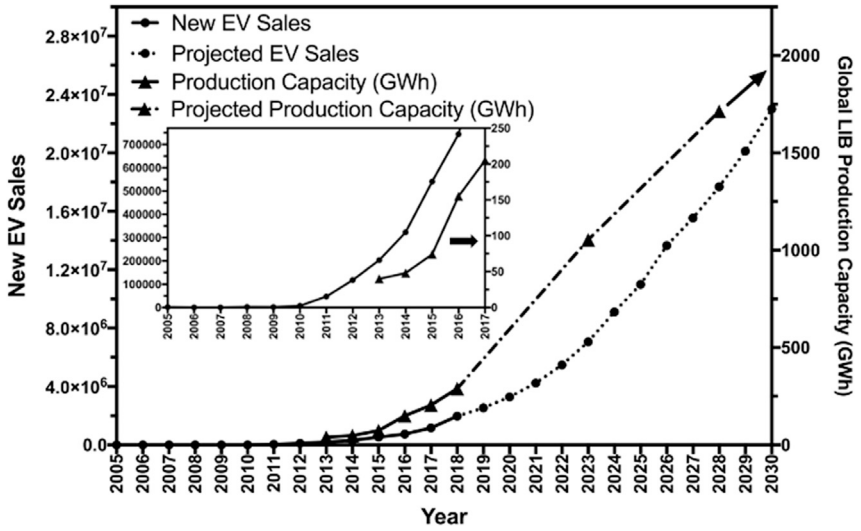

Figure 1. Historical and Projected Global Plug-in EV Sales and LIB Production Capacity
Projected EV sales based on a 21% CAGR (Benchmark Mineral Intelligence, 2019; International Energy Agency, 2019).

concerns over the uneven geographic distribution of the reserves and whether production can meet high demands for lithium by 2050, which can cause price spikes (Speirs et al., 2014; Vikström et al., 2013). On the other hand, reports have indicated that deficits in the cobalt supply could occur as early as 2030 (Alves Dias et al., 2018). As seen in Figures 2A and 2B, cobalt is by far the most valuable metal used in LIBs. In 2010, ~25% of all cobalt produced was used in secondary batteries (LIBs and minor quantity in Ni-MH batteries), which grew to 30% in 2017 and is expected to expand to 53% by 2025 (Azevedo et al., 2018). Moreover, cobalt continues to be an important component in catalysts, integrated circuits, semiconductors, magnetic recording devices, and various high-strength alloys. However, cobalt is scarce and expensive to process, as it is mostly derived from low-concentration by-products of nickel and copper mining. Cobalt is considered a critical resource as ~60% of the worldwide mine production in 2018 originated from copper-cobalt ores in the Democratic Republic of the Congo (DRC), where geopolitical instability and unethical working conditions are well documented and can lead to halting of cobalt exports (Schulz et al., 2017; Tsurukawa et al., 2011). This was apparent in 1978 where civil conflict generated a drastic price spike known as the Cobalt Crisis (Figure 2A).

Moreover, China has dominance over the cobalt supply chain as the world largest producer, supplier, and consumer (Figure 2C). China has heavily invested and acquired foreign cobalt mining operations primarily in the DRC since 2000, which has reduced their net import reliance of raw cobalt from 97% to 68% (Gulley et al., 2019). Considering that China itself may experience cobalt supply deficits by 2030 unless efficient recycling targets are achieved (Zeng and Li, 2015), China's cobalt production will likely be prioritized for domestic battery manufacturers. Continued global reliance on cobalt may lead to competition for raw materials and ensuing conflicts similar to the rare earth metals trade dispute in 2010, which will urge investigations into cobalt-free energy storage technologies (Overland, 2019).

CURRENT COBALT-FREE COMMERCIAL CATHODES

The issue with cobalt resource scarcity was acknowledged early on by LIB pioneers, motivating research into abundant and sustainable cathode chemistries. Goodenough's research group first reported the olivine $LiFePO_4$ (LFP) cathode in 1997, and the path toward commercialization was paved after the development of a carbon-coated nanoparticle morphology to address its poor intrinsic electronic and ionic conductivity (Li et al., 2018b). LFP is attractive owing to its high thermal stability associated with the covalent phosphate moieties, excellent cycle life, flat charge/discharge profile, and high electrochemical stability over ~100% depth of discharge (DOD). However, it has achieved little market traction in Western markets owing to its low energy density and nominal voltage (~3.3 V versus graphite anode), which directly affects the driving range of EVs. However, LFP technology generates significant interest in China owing to its cobalt-free composition and has been developed and adopted by major EV manufacturers, such as the BYD

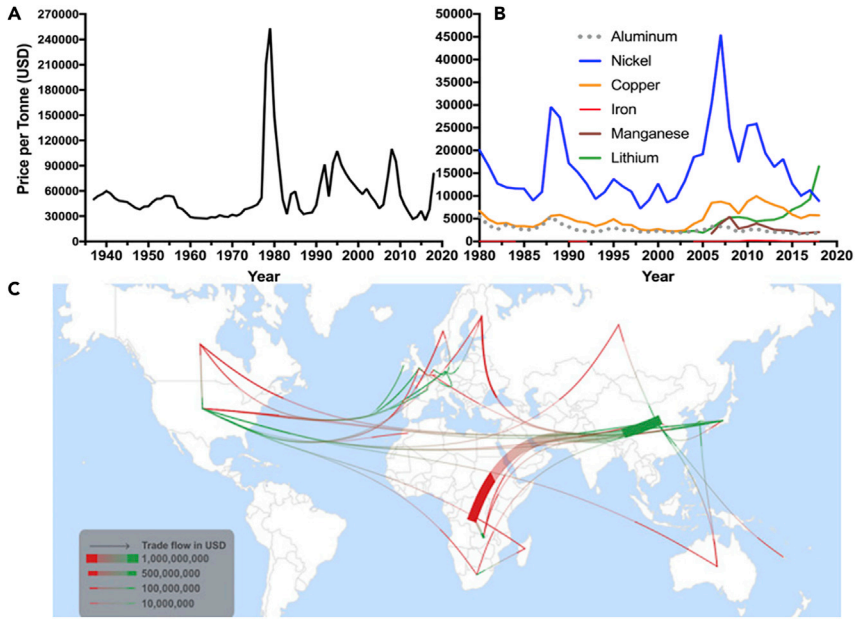

Figure 2. Metal Supply for LIB Components

(A) Historical inflation-adjusted commodity price of cobalt.

(B) Commodity price of other common metals used in LIBs.

(C) Trade flow of raw and processed cobalt. Image adapted with permission from Olivetti et al. (2017).

Company and the Wanxiang Group Corporation. Most electric buses (~99% of the global stock concentrated in China) utilize LFP batteries (International Energy Agency, 2019). Thus, many speculate that LFP will play an important role in public transportation and stationary energy storage, where safety and stability are more critical than the energy density (Zeng et al., 2019). An area of improvement of LFP is lowering the production cost associated with the complex synthesis methods to favor the cost/performance ratio. The electrochemical performance of LFP is highly sensitive to the preparation method, requiring rigorous control of morphology, particle size distribution, coating homogeneity, and reagent purity while ensuring that Fe^{2+} is not oxidized to Fe^{3+} for performance consistencies (Jugović and Uskoković, 2009; Yuan et al., 2011).

Similarly, spinel $LiMn_2O_4$ (LMO) is a commercially relevant cobalt-free cathode that was first reported by Goodenough's group in 1983 (Thackeray et al., 1983). The host structure enables 3D solid-state diffusion of Li^+, resulting in high LIB rate performances. However, its main setback is the low practical capacity and cycle stability caused by the presence of Mn^{3+}. The electronic configuration of Mn^{3+} (t_{2g}^3-e_g^1) induces Jahn-Teller distortion, which can cause lattice changes from the cubic to tetragonal phase and constrict Li^+ diffusion (Yamada, 1996). The distortion is more pronounced when discharging at high rates as Li^+ is more concentrated at the surface of the LMO particles, which pronounces the distortion, resulting in particle cracking and exfoliation (Li et al., 2009). Moreover, Mn^{3+} generates soluble Mn^{2+} based on the disproportionation reaction: $2Mn^{3+}(solid) \rightarrow Mn^{4+}(solid) + Mn^{2+}(solution)$. Suppression of Jahn-Teller distortion has commonly been addressed by partially substituting Mn with other cations to reduce the amount Mn^{3+}(Capsoni et al., 2003; Kim and Lee, 2007; Li et al., 2009), while various coatings have been explored to suppress the dissolution of Mn (Guan et al., 2011). Ultimately, the poor reliability of LMO limits it toward niche applications.

LAYERED MIXED-TYPE CATHODES

On the other hand, layered mixed-type transition metal oxide cathodes are the most suitable to reach the high-energy requirements for EVs. Among the NMC-type compositions, $LiNi_{1/3}Mn_{1/3}Co_{1/3}O_2$ (NMC111) is the most established and known for its stability and safety (Belharouak et al., 2003; Noh et al., 2013). In this solid solution, Mn^{4+} is electrochemically inactive and assists with thermal and electrochemical stability, whereas Co^{3+} contributes to electronic conductivity and suppresses cation mixing between Ni^{2+} and Li^+ (Myung et al., 2017; Zeng et al., 2018). Capacity is primarily dependent on the Ni^{2+}/Ni^{4+} redox couple

with contribution from Co^{3+}/Co^{4+} at higher voltages. Motivated by the higher capacities (at 4.3 V versus Li/Li^+ upper cut-off) and lower cobalt content, there is ongoing commercial development to substitute NMC111 (~160 mAh g^{-1}, 20.4 wt % Co) with $LiNi_{0.6}Mn_{0.2}Co_{0.2}O_2$ (NMC622, ~180 mAh g^{-1}, 12.2 wt % Co) and $LiNi_{0.8}Mn_{0.1}Co_{0.1}O_2$ (NMC811, ~200 mAh g^{-1}, 6.1 wt % Co) (Myung et al., 2017). The increase in nickel content raises the capacity at the expense of cycle and thermal stability (Noh et al., 2013). With higher nickel content, the degree of (de)lithiation increases, resulting in anisotropic lattice volume changes that contribute to particle cracking (Li et al., 2019b). Nickel-rich cathodes also suffer from increased moisture sensitivity, Li^+/Ni^{2+} cation mixing, electrolyte side reactions (solvent oxidation from Ni^{4+}), and phase transitions toward spinel and rock-salt structures along with oxygen evolution at elevated temperatures and voltages (Myung et al., 2017). A promising approach to address these issues is to synthesize NMC as micron-scale single crystal particles. Compared with polycrystalline NMC that comprises 10- to 15-μm-size agglomerates of nanoparticles, the single-crystal morphology has a minimal number of grain boundaries and thus can mitigate particle cracking and side reactions with the electrolyte (Kim, 2012; Li et al., 2017). A more popular approach in the literature involves synthesizing core-shell NMC, where the core is Ni-rich and enhances capacity, whereas the shell is Mn-rich and can alleviate volume expansion and protect the core from electrolyte reactions (Sun et al., 2006, 2009, 2010, 2012). Similarly, $LiNi_{0.8}Co_{0.15}Al_{0.05}O_2$ (NCA) is a "low-cobalt" (9.2 wt % Co) cathode composition known to display a similar energy density to NMC811, although with better cycle retention but poorer thermal stability (Xia et al., 2018).

These developments in high-energy cathodes with lower cobalt content raises the question as to whether they are enough to sustain long-term and large-scale LIB applications. Olivetti et al. projected cobalt demand assuming that the LIBs implemented in EVs comprise 50% NMC111, 35% NMC622, and 15% NMC811 (Olivetti et al., 2017). Their conservative projected demand was based on a 36% compound annual growth rate (CAGR) of EV sales and assuming an average battery pack size of 75 kWh, whereas the aggressive projection assumed 10 million EV sales (10% of all vehicles) in 2025. These scenarios correspond to 136 and 336 kt of cobalt demand. On the other hand, the projected expansions in cobalt supply was 180 and 290 kt for the conservative and aggressive projections, respectively. Similarly, the International Energy Agency projected a cobalt demand of 170 $\pm$ 60 kt in 2030 based on currently announced policy ambitions, assuming that the LIB chemistry then comprises 10% NCA, 40% NMC622, and 50% NMC811 (International Energy Agency, 2019). These findings indicate that, even while implementing low-cobalt cathodes in EVs, cobalt supply strains could occur in the near future if aggressive EV targets are met. It is also worth mentioning that high-nickel LIBs will need to be replaced more frequently owing to their lower cycle life. Furthermore, this projection does not account for sudden constraints in supply due to political issues and other risk factors as discussed earlier.

LIB metal recycling can help address the resource constraints. However, owing to the continuous expansions in battery production (Figure 1), production is expected to substantially outweigh the amount of end-of-life batteries entering the waste stream over the foreseeable future. Furthermore, LIB recycling activities are concentrated in China, whereas infrastructure elsewhere consists of select private facilities focused on recovering high-value cobalt (Wang et al., 2014). Although the recycling of end-of-life $LiCoO_2$ batteries in portable electronics is highly feasible and profitable, there are significant technical challenges and decreased financial motivation in recycling mixed-metal LIBs in EVs that will dominate the waste stream over the next decades (Or et al., 2020). Furthermore, the dismantling of cells from EV battery packs is currently not economically feasible. Although the concept of repurposing end-of-life battery packs (~80% capacity retained) toward stationary energy storage has been proposed, it is not well developed (Ahmadi et al., 2014). Worldwide realization of LIB recycling will require legislation and political pressure, likely in the form of economic incentives (e.g., refundable deposits with LIB purchases), public education, landfill disposal regulations, and defined responsibilities on the collection and disposal of LIBs for consumers, retailers, and EV and battery manufacturers. Taken together, it is evident that cobalt-free cathodes are required for sustainable long-term applications of LIBs.

COBALT-FREE LAYERED CATHODES

Improving nickel-rich layered $LiNi_{1-x}M_xO_2$ (M = Mn, Al, and/or Co)-type materials is one of the most promising approaches to developing cathodes for LIBs with reduced reliance on cobalt and has attracted a considerable amount of research effort over the past several years (Aishova et al., 2020; Cheng et al., 2019; Cormier et al., 2019; Li et al., 2019a; Xu et al., 2017; Zhang et al., 2019). Nickel-rich cathodes such as NMC811 and NCA are a step forward to developing completely cobalt-free $LiNiO_2$-based materials

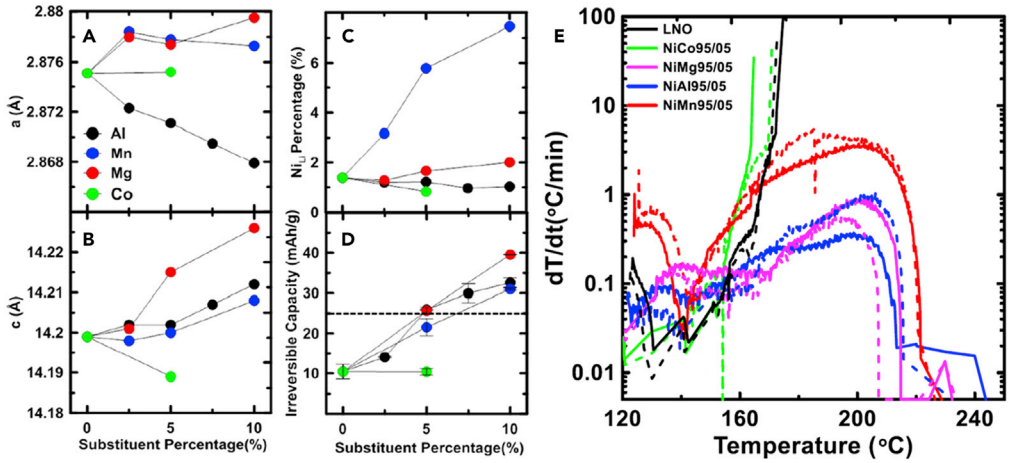

Figure 3. Unit Cell Dimensions

(A and B) (A) a-axis and (B) c-axis as a function of substituent content.

(C) Percentage of Ni found within the Li layer (Ni_{Li}) as a function of substituent content.

(D) Irreversible capacity [mAh g^{-1}] as a function of substituent content.

(E) Self-heating rate (SHR) for de-lithiated $LiNiO_2$ and $LiNi_{0.95}M_{0.05}O_2$ (M = Al, Co, Mg, Mn) charged to 230 mAh g^{-1} as a function of temperature between 120°C and 250°C. Images adapted with permission from Li et al. (2019a).

(LNO) capable of delivering high energy density in line with performance targets set for future EVs. However, thermal instability (Dahn et al., 1994; Guilmard et al., 2003a, 2003b) and structural decomposition leading to poor electrochemical performance (Bianchini et al., 2020; Croy et al., 2019) are primary barriers inhibiting further applications of cobalt-free layered cathodes over existing materials in modern LIBs. Intermixing of Ni^{2+}/Li^{+} cations during cycling is one of the main degradation pathways, causing localized formations of an inactive rock-salt phase that worsen during subsequent cycles. As seen in NMC and NCA-type compositions, substitution of nickel for cobalt is thought to be an effective method of stabilizing Ni^{2+} ions within the transition metal layer, thereby reducing the degree of cation mixing (Croy et al., 2019). However, recent work has called into question whether cobalt is necessary or if a similar effect could be achieved using other metal substituents (e.g. Al, Mn, or Mg) (Li et al., 2019a). Capacity degradation in layered transition metal oxides also occurs through the formation of microcracks in secondary particles owing to uneven volumetric expansion within the lattice (Makimura et al., 2012). The propagation of microcracks in secondary particles increases the available surface area for the formation of a passivated solid-electrolyte interface (SEI), causing an increased consumption of lithium that leads to irreversible capacity reduction (Watanabe et al., 2014). Additionally, intergranular cracking causes a loss of contact between the grains of secondary particles, giving rise to an increased impedance in the battery. The deleterious phase transition from hexagonal 2 (H2) → hexagonal 3 (H3) with low reversibility is well known to occur at high degrees of delithiation within Ni-rich layered cathodes and is thought to be a major contributor to particle cracking due to sharp volumetric contractions of the unit-cell (*c*-axis) (Li et al., 2015, 2018a; Weber et al., 2017). High-temperature operation (≥50°C) of the material can enhance the rate performance for cobalt-free compositions; however, operation above 30°C can accelerate structural degradation and thus should not be relied upon (Aishova et al., 2020; Ma et al., 2018; Sun et al., 2015). These issues need to be resolved in order to drive nickel-rich and cobalt-free layered oxide cathodes toward commercialization in next-generation EVs.

Recent work from Li et al. has cast uncertainty in previously theorized contributions of cobalt substitution in nickel-rich layered cathodes by investigating various compositions of $LiNi_{1-x}M_xO_2$ (M = Al, Co, Mg, or Mn; x = 0.05 or 0.1) (Li et al., 2019a). Similar amounts of Ni^{2+} in the Li^{+} layer (Ni_{Li}) were found for both $LiNi_{0.90}Co_{0.05}Al_{0.05}O_2$ and LNO substituted with 5 mol% Al, Mg, or Co (Ni_{Li} ~1%), indicating that Co does not provide a significant reduction of cation mixing compared with Al or Mg (Figure 3C). The presence of Mg caused a preferential positioning of Li atoms in vertex-sharing sites within the layers above and below the substituent. This caused two Li atoms to become "locked in" for every one Mg atom, reducing the interlayer repulsion that is associated with detrimental phase changes in the cathode. However, this also reduced the reversible charge capacity, as two Li atoms became inactive for every Mg atom in the structure.

Subsequently, $LiNi_{0.95}Mg_{0.05}O_2$ delivered an initial charge capacity of 205 mAh g^{-1} (~10% loss) between 3.0 and 4.3 V versus Li^+/Li at 10 mA g^{-1}, compared with 219 mAh g^{-1} and 223 mAh g^{-1} for $LiNi_{0.95}Mn_{0.05}O_2$ and $LiNi_{0.95}Al_{0.05}O_2$, respectively. This report further indicated that there was no noticeable improvement from $LiNi_{0.95}Co_{0.05}O_2$ in structural stability throughout cycling, as minimal variation in unit-cell volume as a function of Li content (x in $Li_{1-x}MO_2$) was observed in all substituted samples tested (Figures 3A and 3B). The initial discharge capacity (IDC) and cycle retention of $LiNi_{0.95}Al_{0.05}O_2$ was similar to traditional NCA, with ~95% of the initial capacity retained after 50 cycles at 10 mA g^{-1}, whereas $LiNi_{0.95}Mg_{0.05}O_2$ displayed the best cycle retention of 97% after 50 cycles albeit with lower IDC, implying that cobalt is not required for Ni-rich materials to attain acceptable long-term capacity retention. However, the rate performance of these compositions was not assessed. In addition, cobalt substitution did not improve thermal stability over conventional LNO with self-heating rates (SHRs) > 20°C min^{-1} at 160°C, whereas Al and Mg demonstrated noticeable benefit by keeping SHR <1°C min^{-1} over the range of 120°C–240°C (Figure 3E). This report challenged the necessity of cobalt in layered oxides and highlighted the comparable performance in cathodes with other metal dopants.

The impact of various substituents on both Co-free Ni- and Mn-rich compounds has been studied over the last several years, where cation doping with Mg^{2+}, Al^{3+}, Fe^{3+}, Na^+, etc. has enabled advancements of the overall electrochemical performance and safety of these compounds (Cheng et al., 2019; Dong et al., 2013; Guilmard et al., 2003c; Mohan and Kalaignan, 2013; Wang et al., 2013). In addition to Li et al., critical progress has been made understanding the relationship among the cathode dopant, thermal stability, and reactivity with the electrolyte. Cormier et al. confirmed that thermal stability is improved in substituted $LiNi_xM_{1-x}O_2$ (M = Mn, Mg, Al, or Co; x = 0 or 0.05) (Cormier et al., 2019). The substituent can enable the cathode to maintain a greater Li content at the end of charge (~4.4 V versus Li^+/Li), which reduces the propensity for oxygen evolution and stabilizes the structure. The stabilized oxides display substantially less aggressive reactions with the electrolyte, causing the SHR to occur at much higher temperatures (220°C) than $LiNi_{0.95}Co_{0.05}O_2$/LNO (160°C).

In another study, Aishova et al. investigated the electrochemical performance of $LiNi_{0.9}Mn_{0.1}O_2$ (NM90), a nickel-rich derivative of the most widely studied cobalt-free composition $LiNi_{0.5}Mn_{0.5}O_2$ (Aishova et al., 2020). The authors confirmed that NM90 exhibits a higher degree of cation mixing (Ni_{Li} = 3.35%) than both cobalt-containing compounds, $LiNi_{0.9}Mn_{0.05}Co_{0.05}O_2$ (Ni_{Li} = 1.77%) and $LiNi_{0.9}Co_{0.1}O_2$ (Ni_{Li} = 0.67%). No difference in the IDC (236 mAh g^{-1}) was observed among the samples from 2.7–4.4 V versus Li^+/Li at 0.1 C, and capacity retention improved as a function of Mn content, with NM90 retaining 93% after 100 cycles. Inactive Mn^{4+} ions are theorized to stabilize the structure upon delithiation, evidenced in an upshift of the redox potential associated with the destructive H2 → H3 phase transition. Broadening of the dQ/dV peak was also observed, indicating that the lattice volumetric change was spread over a wider voltage range, allowing relief of non-uniform strain in the lattice of NM90. Additionally, the fracture strength of secondary particles in materials with higher Mn content was increased, with 25% higher strength in NM90 (175 MPa) than $LiNi_{0.9}Mn_{0.05}Co_{0.05}O_2$ (140 MPa) and nearly double that of $LiNi_{0.9}Co_{0.1}O_2$ (95 MPa). Both of these mechanisms demonstrate an important role in the cycle stability of the Mn-substituted $LiNiO_2$.

Further improvements to the cyclability of cobalt-free layered oxides were reported by de Bosse et al. who observed that preparation of a Li-rich layered oxide material with O2-type oxide packing could suppress the H2→H3 phase transition by preventing the previously mentioned antisite exchange (de Boisse et al., 2018). A unique synthesis methodology was employed to achieve this structure, involving the ionic exchange of Na^+ in P2-$Na_{0.83}[Li_{0.19}Mn_{0.73}Ni_{0.08}]O_2$ for Li^+ in molten salt, yielding Li-rich O2-$Li_{1.19-y}Mn_{0.73}Ni_{0.08}O_2$. The resulting O2-type LMNO delivered an IDC of 240 mAh g^{-1} from 2.0–4.8 V versus Li^+/Li at 0.05 C. However, the work also indicated an excellent capacity retention compared with the O3-type analogs, retaining >90% of the initial capacity after 50 cycles. This work suggests that structural adjustments through modifying synthesis procedures could be a key strategy to developing next-generation cobalt-free cathode materials.

Surface treatments and coatings have also been investigated as a solution to improve the stability and rate performance of Co-free cathodes. In general, their ability to act as a protective barrier between electrolyte and active material, and a scavenger to reduce the acidity of non-aqueous electrolytes can substantially restrict metal ion dissolution during cycling (Chong et al., 2016; Li et al., 2012; Wu et al., 2017; Zhang

et al., 2012). One of the most promising studies recently was presented by Deng et al. who designed a modified F- B-rich SEI on $LiNiO_2$ with the addition of a small amount of difluoro (oxalato) borate (LiDFOB) in the electrolyte (Deng et al., 2019). The SEI formed as a robust and compact layer that mitigated the dissolution of Ni as well as the irreversible transformation to the unwanted NiO rock salt phase by protecting the surface from reacting with the by-products generated from the oxidation of electrolyte at high voltage. This material showed a high IDC of 216 mAh g^{-1} from 2.0–4.4 V versus Li^+/Li with an exceptional cycling performance of 94% after 100 cycles and 80% retention after 400 cycles. In comparison, the LNO cycled without the LiDFOB additive retained only 18% of the initial capacity after 100 cycles.

The design and engineering of spatially partitioned nanostructures for cobalt-free cathodes is an interesting new strategy that has seen some research activity in the past few years (Li et al., 2016b; Pan et al., 2018; Xu et al., 2019). Similar to the work conducted in Ni-rich NMC, the use of core-shell and gradient core-shell structures for cobalt-free materials was preliminarily investigated by Zhang et al. (2019). The authors prepared a $LiNiO_2$ core with a $LiNi_{1-x}M_xO_2$ shell (M = Al, Mg, Mn), finding that the core-shell materials delivered a high IDC of 194 mAh g^{-1} ($LiNi_{0.83}Mg_{0.17}O_2$ shell) and 230 mAh g^{-1} ($LiNi_{0.83}Al_{0.17}O_2$ $LiNi_{0.83}Mn_{0.17}O_2$ shell) from 3.0–4.35 V versus Li^+/Li at 0.2 C. The LNO-$LiNi_{0.83}Mg_{0.17}O_2$ and LNO-$LiNi_{0.83}Mn_{0.17}O_2$ core-shell electrodes retained 94% and 92% of their initial capacity, respectively, after 55 cycles, whereas the LNO-$LiNi_{0.83}Al_{0.17}O_2$ electrode retained 93% of its initial capacity after 55 cycles and 69% after 400 cycles at 0.2 C. Despite the high capacities, it was found that the metal substituents diffused from the shell to the core structure during sintering, suggesting that the benefit of the core-shell structure was not fully realized. Nevertheless, the report demonstrates the promising nature of this approach and suggests room for improvement through a more optimized synthesis pathway. Wang et al. prepared Li-rich $Li_{1.2}Mn_{0.6}Ni_{0.2}O_2$ with a porous nanoflake network through a resorcinol-formaldehyde assisted sol-gel method (Wang et al., 2017). The specific surface area of the nanoflake material was 6.9 m^2 g^{-1}, which is a notable improvement over spherical analogs at 1.5 m^2 g^{-1} (Li et al., 2016a). The high surface area facilitates the diffusion of lithium leading to an elevated rate performance, with discharge capacities of 273 mAh g^{-1} at 0.1 C and 196 mAh g^{-1} at 2 C from 2.0–4.8 V versus Li^+/Li. A potential concern with this material would be the electrochemical stability due to the high surface area available for SEI formation and Li consumption; however, a stable capacity was reported with 93% retention after 150 cycles at 2 C indicating that the stability of the material was not negatively impacted by the modified morphology.

CATION DISORDERED ROCK SALT CATHODES

Disordered rock salts are an emerging class of high-energy-density cathode materials. Disordered materials have been largely overlooked as they are associated with an electrochemically inactive phase formed within conventional layered materials during cycling. However, recent reports indicate that disordered materials can offer higher capacity than other modern LIB cathodes and suppress common failure mechanisms observed in layered oxide materials. Conventional layered materials exhibit distinct Li layers separated by the transition metal (TM) sublattice, whereas disordered materials have Li/TM intermixed in random fashion at octahedral sites within the same cubic close packed (ccp) lattice (Figures 4A and 4B). Additionally, the cation disordered lattice does not suffer from structural degradation caused by cation mixing that is observed in layered structures (Lee et al., 2014).

Li^+ diffusion in disordered rock-salts proceeds primarily through channels with no face-sharing TM ions (0-TM), whereas the typical pathway found in layered materials with one face-sharing TM ions (1-TM) is nearly inactive in disordered materials. The 0-TM channels in disordered materials have a low diffusion barrier, indicating facile movement of Li^+ within the atomic structure; however, the infrequency of these channels in the disordered structure prevents the formation of a continuous percolating network and lowers the probability of macroscopic diffusion of Li^+. Heterogeneity of the material also implies that localized cation ordering influences the Li^+ conduction pathways, further contributing to disruptions of the continuous percolation network (Kan et al., 2018). Thus, disordered materials suffer from poor rate capability owing to these sluggish Li^+ diffusion pathways and the presence of high-valence transition metals that cannot be oxidized and thus do not contribute to charge compensation (e.g., Nb^{5+}).

Disordered rock salts suffer structural degradation primarily through the irreversible release of surface-level oxygen at high voltages (>4.3 V versus Li^+/Li). The O^{2-}/O_2^{2-} anions are used for charge compensation of Li^+, enabling enrichment of Li content in the cathode. Utilization of the oxygen redox for charge compensation is critical toward achieving the high reversible capacities in disordered rock salts, which can be

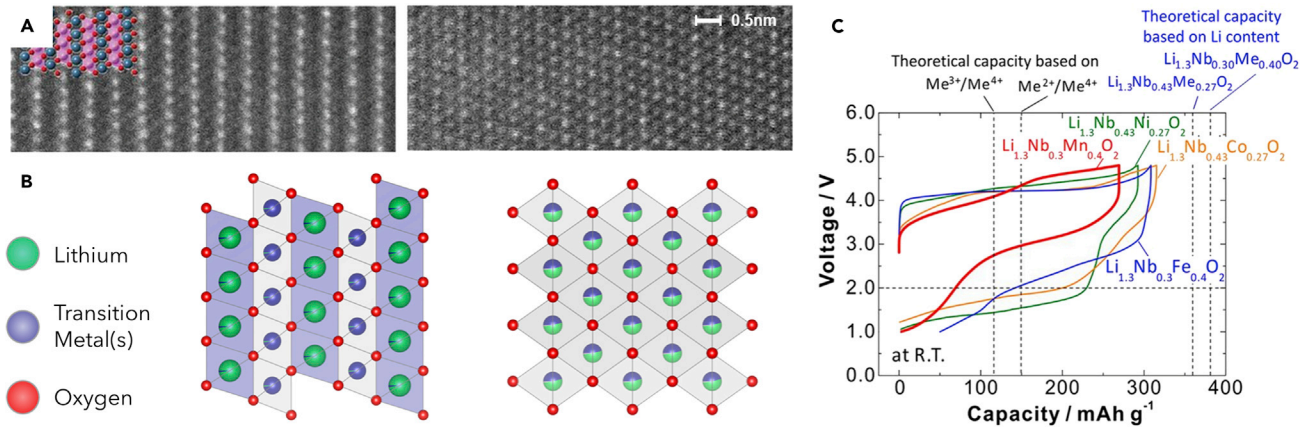

Figure 4. Physical and Electrochemical Comparison of Layered Transition Metal Oxide and Cation Disordered Rock-salt Cathode Materials

(A) Scanning transmission electron microscopy (STEM) images along [010] zone axis for left: layered $Li_{1.211}Mo_{0.467}Cr_{0.3}O_2$ before cycling and right: fully disordered $Li_{1.211}Mo_{0.467}Cr_{0.3}O_2$ after 10 cycles. Images adapted with permission from Lee et al. (2014).

(B) Schematic of the general crystal lattice for left: conventional layered transition metal oxides; right: cation disordered transition metal oxides.

(C) Electrochemical performance (V versus Capacity) of cation disordered rock salt electrodes with various metal substituents (i.e., Ni, Mn, Fe, Co) at room temperature between 1.0 and 4.8 V versus Li^+/Li at 10 mA g^{-1} rate. Image adapted with permission from Yabuuchi et al. (2015).

observed when charging above 4.3 V versus Li^+/Li (Figure 4C). However, the release of oxygen as a reactive radical species (O^-/O_2^{2-}) initiates formation of a resistive interfacial layer through electrolyte decomposition, and structural degradation is further induced by vacancy defects from oxygen release (Cambaz et al., 2019; Luo et al., 2016; Yan et al., 2019). Currently, long-term capacity retention has not been reported for these materials, but the high theoretical energy densities have galvanized considerable research effort to alleviate these failure mechanisms.

Lee et al. investigated the partial substitution of O^{2-} for F^- in a $Li_{1.3}Mn_{0.4}Nb_{0.3}O_2$ disordered rock salt to facilitate the use of lower valence Mn^{2+} in the structure for higher theoretical capacity and reduced oxygen loss (Lee et al., 2018). The unsubstituted material employs the Mn^{3+}/Mn^{4+} redox, leading to low theoretical capacity; however, F^- substitution reduced the valence of Mn in the structure allowing for use of the Mn^{2+}/Mn^{4+} redox couple (270 mAh g^{-1}). As a result, the reliance on oxygen redox reactions to achieve capacities >300 mAh g^{-1} is mitigated. The diminished use of the anionic redox minimized oxygen release, providing higher cycling stability to the cathode and lower polarization (Lee et al., 2017). Surface modification of disordered rock salts through minor doping with heavy elements (e.g., Os, Sb, Ru, Ir, Ta) was reported by Shin et al. to improve oxygen retention at the surface (Shin et al., 2018). Larger-sized dopants tend to segregate at the surface, and cations exhibiting stronger hybridization with neighboring oxygen atoms improved oxygen retention. Slight improvements to electrochemical stability were observed, with a significant reduction in irreversible oxygen loss in doped materials. In general, mitigating the loss of oxygen is seen as the key to achieving higher cycle stability in disordered rock salt materials. Despite the promising energy metrics and initial efforts to improve electrochemical stability, rate performance continues to hinder deployment of disordered rock salts in modern applications. Future research on this topic is critical to resolving this issue and pushing the material toward commercialization in next-generation LIBs.

CONVERSION CATHODES

Finally, conversion electrodes are an interesting next-generation technology that demonstrates ultra-high gravimetric capacity owing to their reaction with 2–3 stoichiometric equivalents of Li^+ while comprising low-cost materials (Figure 5A). However, they possess low theoretical potentials (often <3.5 V versus Li^+/Li). The most studied and promising material is the sulfur cathode (S/Li_2S), which has already been implemented in lightweight batteries for niche aerospace applications. Metal fluorides (MF_2, M = Fe, Mn, Cu, Co, or Ni) are also promising as they demonstrate higher theoretical potentials and can potentially compete with the energy density NMC/NCA-type cathodes when paired with a graphite anode (Wu and Yushin, 2017). However, severe drawbacks must be overcome, particularly the discrepancy between the theoretical and practical potential, poor intrinsic conductivity and diffusion kinetics, and low reversibility. One notable cause of poor reversibility is the high solubility of the cathode materials, resulting in dissolution and subsequent

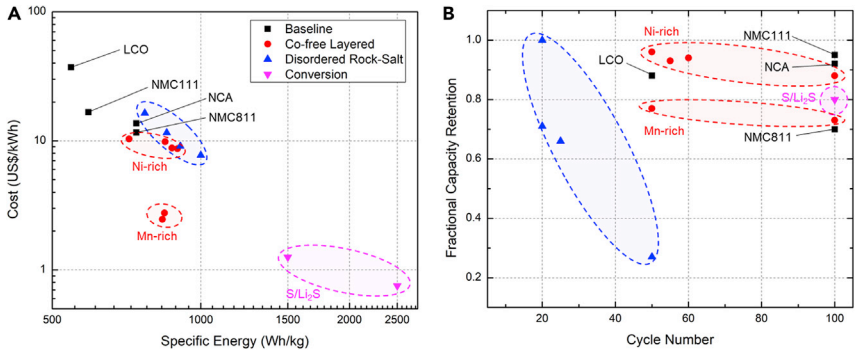

Figure 5. Comparison of Selected Promising Co-free Cathode Compositions in the Literature

Commercial cathodes (LCO, NMC, and NCA) also included for comparison.

(A) Specific energy (Wh kg^{-1}) relative to material cost (US$ kWh^{-1}). Cost does not account for production, manufacturing, or synthesis approach. Material cost obtained from the metal commodity price in June 2020.

(B) Comparison of demonstrated cycle performance. Data used in calculations shown in Table S1.

redeposition at the anode or cathode, which can throttle capacity and negatively influence the SEI makeup. In addition, the lithiation/delithiation cycles are associated with significant volume changes, resulting in particle fracturing, particle disconnection, and electrode swelling. There have been many studies published to mitigate these issues, particularly for the sulfur cathode, where promising performance benchmarks with respect to cycle life (<20% degradation over 1,000 cycles) and rate capability (>80% capacity retention at 1 C) have been achieved (Kang et al., 2016). However, many techniques are complex and costly, and have poor scalability. Engineering innovations are also required to optimize cell fabrication for new technologies. Furthermore, to achieve notable expansions in energy density, the cathode must be paired with a high-capacity anode, namely, silicon or lithium metal. These anode materials present similar challenges with respect to stability and safety. Taken together, it is difficult to predict when conversion cathodes will become commercially viable.

CONCLUSION AND PERSPECTIVES

Concerns over cobalt scarcity has been understood as an issue for several decades; however, the use of modern "low-cobalt" materials (e.g., NMC622, NMC811, NCA) is not a sufficient mitigation strategy to this issue, as supply strains could still arise as early as 2025 if aggressive EV sales targets are met. LIB recycling is a direct solution to cobalt recovery, but technical complications with battery pack disassembly and the mixed-metal components constrict its use. Currently, only China is positioned for LIB recycling and global implementation requires economic incentives, improved public education, and cooperation with LIB manufacturers. A more effective and lasting solution for the sustainable future of LIBs is the development of cobalt-free cathode materials.

Layered transition metal oxides based on $LiNiO_2$ have attracted significant research efforts for their high energy density. Inherent issues associated with the poor cycle stability (Figure 5B) of nickel-rich and cobalt-free layered cathodes include the volume expansion and particle cracking owing to the higher Li^+ utilization (i.e., capacity), Ni^{2+}/Li^+ cation mixing, increased electrolyte oxidation, and lower thermal stability and rate performances. Partial substitution of Ni with Mn, Al, and Mg helps improve the thermal stability and cycle performance through the suppression of phase changes and particle cracking. Doping $LiNiO_2$ with Mn does not reduce the IDC, although it increases the degree of Ni^{2+}/Li^+ cation mixing. However, Al and Mg can help suppress Ni^{2+}/Li^+ mixing at the expense of the IDC. For optimal performance, the cation doping strategy can be coupled with morphology control (e.g., single crystal particles to suppress cracking), coatings that improve interparticle conductivity or provide a protective barrier against electrolyte side reactions and suppress oxygen evolution, and adjustments to the oxide packing structure to suppress phase changes. Research in this direction provides the most practical and short-term path toward the commercialization of cobalt-free cathodes. On the other hand, cation disordered rock salt cathodes are an emerging material class with high energy density (up to ~1,000 Wh kg^{-1}). Future research for this material should be focused on improving the rate performance (e.g., through surface treatments) and minimizing oxygen loss (e.g., doping, core-shell structures) to extend cycle life. With increasing effort, the

development of cobalt-free cathode materials can address the cobalt scarcity issue and sustain large-scale deployments of LIBs toward EVs and stationary energy storage.

Limitations of the Study

In Figure 5, data were obtained from referenced literature sources in half-cell configuration (versus Li/Li^+ anode)—performance may not be representative of updated industry benchmarks. The material cost calculation was based on the metal commodity price from June 2020 and does not account for production, manufacturing, or synthesis approach.

Resource Availability

Lead Contact

Further information and requests should be directed to and will be fulfilled by the Lead Contact, Zhongwei Chen (zhwchen@uwaterloo.ca).

Materials Availability

This study did not generate any new materials.

Data and Code Availability

Any data utilized in this study can be found in the main manuscript and Supplemental Information.

METHODS

All methods can be found in the accompanying Transparent Methods supplemental file.

SUPPLEMENTAL INFORMATION

Supplemental Information can be found online at https://doi.org/10.1016/j.isci.2020.101505.

ACKNOWLEDGMENTS

The authors gratefully acknowledge financial support from the Natural Sciences and Engineering Research Council of Canada (NSERC) and the University of Waterloo.

AUTHOR CONTRIBUTIONS

Writing – Original Draft, S.W.D.G. and T.O.; Writing – Review & Editing, S.W.D.G., T.O., and Z.C.; Supervision, Z.C.

REFERENCES

Ahmadi, L., Fowler, M., Young, S.B., Fraser, R.A., Gaffney, B., and Walker, S.B. (2014). Energy efficiency of Li-ion battery packs re-used in stationary power applications. Sustain. Energy Technol. Assess. *8*, 9–17.

Aishova, A., Park, G.T., Yoon, C.S., and Sun, Y.K. (2020). Cobalt-free high-capacity Ni-rich layered Li[Ni0.9Mn0.1]O2 cathode. Adv. Energ. Mater. *10*, 1–9.

Alves Dias, P., Blagoeva, D., Pavel, C., and Arvanitidis, N. (2018). Cobalt: Demand-Supply Balances in the Transition to Electric Mobility (Publications Office of the European Union).

AVICENNE Energy (2017). The Rechargeable Battery Market and Main Trends 2016 – 2025.

Azevedo, M., Campagnol, N., Hagenbruch, T., Hoffman, K., Lala, A., and Ramsbottom, O. (2018). Lithium and Cobalt - a Tale of Two Commodities (McKinsey Co. Met. Min).

Belharouak, I., Sun, Y.K., Liu, J., and Amine, K. (2003). Li(Ni1/3Co1/3Mn1/3)O2 as a suitable cathode for high power applications. J. Power Sources *123*, 247–252.

Benchmark Mineral Intelligence (2019). Lithium Ion Megafactory Assessment.

Berckmans, G., Messagie, M., Smekens, J., Omar, N., Vanhaverbeke, L., and Van Mierlo, J. (2017). Cost projection of state of the art lithium-ion batteries for electric vehicles up to 2030. Energies *10*, 1314.

Bianchini, M., Fauth, F., Hartmann, P., Brezesinski, T., and Janek, J. (2020). An: in situ structural study on the synthesis and decomposition of LiNiO2. J. Mater. Chem. A *8*, 1808–1820.

Cambaz, M.A., Vinayan, B.P., Geßwein, H., Schiele, A., Sarapulova, A., Diemant, T., Mazilkin, A., Brezesinski, T., Behm, R.J., Ehrenberg, H., and Fichtner, M. (2019). Oxygen activity in Li-rich disordered rock-salt oxide and the influence of LiNbO3 surface modification on the electrochemical performance. Chem. Mater. *31*, 4330–4340.

Cano, Z.P., Banham, D., Ye, S., Hintennach, A., Lu, J., Fowler, M., and Chen, Z. (2018). Batteries and fuel cells for emerging electric vehicle markets. Nat. Energ. *3*, 279–289.

Capsoni, D., Bini, M., Chiodelli, G., Massarotti, V., Mustarelli, P., Linati, L., Mozzati, M.C., and Azzoni, C.B. (2003). Jahn–Teller transition in Al3+ doped LiMn2O4 spinel. Solid State Commun. *126*, 169–174.

Cheng, X., Wei, H., Hao, W., Li, H., Si, H., An, S., Zhu, W., Jia, G., and Qiu, X. (2019). A cobalt-free Li(Li 0.16 Ni 0.19 Fe 0.18 Mn 0.46)O 2 cathode for lithium-ion batteries with anionic redox reactions. ChemSusChem *12*, 1162–1168.

Chong, S., Chen, Y., Yan, W., Guo, S., Tan, Q., Wu, Y., Jiang, T., and Liu, Y. (2016). Suppressing capacity fading and voltage decay of Li-rich layered cathode material by a surface nano-protective layer of CoF2 for lithium-ion batteries. J. Power Sources *332*, 230–239.

Cormier, M.M.E., Zhang, N., Liu, A., Li, H., Inglis, J., and Dahn, J.R. (2019). Impact of dopants (Al,

Mg, Mn, Co) on the reactivity of Li x NiO 2 with the electrolyte of Li-ion batteries. J. Electrochem. Soc. *166*, A2826–A2833.

Croy, J.R., Long, B.R., and Balasubramanian, M. (2019). A path toward cobalt-free lithium-ion cathodes. J. Power Sources *440*, 227113.

Dahn, J.R., Fuller, E.W., Obrovac, M., and von Sacken, U. (1994). Thermal stability of LixCoO2, LixNiO2 and λ-MnO2 and consequences for the safety of Li-ion cells. Solid State Ion. *69*, 265–270.

de Boisse, B.M., Jang, J., Okubo, M., and Yamada, A. (2018). Cobalt-free O2-type lithium-rich layered oxides. J. Electrochem. Soc. *165*, A3630–A3633.

Deng, T., Fan, X., Cao, L., Chen, J., Hou, S., Ji, X., Chen, L., Li, S., Zhou, X., Hu, E., et al. (2019). Designing in-situ-formed interphases enables highly reversible cobalt-free LiNiO2 cathode for Li-ion and Li-metal batteries. Joule *3*, 2550–2564.

Dong, X., Xu, Y., Xiong, L., Sun, X., and Zhang, Z. (2013). Sodium substitution for partial lithium to significantly enhance the cycling stability of Li2MnO3 cathode material. J. Power Sources *243*, 78–87.

Few, S., Schmidt, O., Offer, G.J., Brandon, N., Nelson, J., and Gambhir, A. (2018). Prospective improvements in cost and cycle life of off-grid lithium-ion battery packs: an analysis informed by expert elicitations. Energy Policy *114*, 578–590.

Grand View Research (2017). Lithium-Ion Battery Market Analysis by Product (Lithium Cobalt Oxide, Lithium Iron Phosphate, NCA, LMO, LTO, Lithium Nickel Manganese Cobalt (NMC)), by Application, and Segment Forecasts, pp. 2018–2025.

Gruber, P.W., Medina, P.A., Keoleian, G.A., Kesler, S.E., Everson, M.P., and Wallington, T.J. (2011). Global lithium availability. J. Ind. Ecol. *15*, 760–775.

Guan, D., Jeevarajan, J.A., and Wang, Y. (2011). Enhanced cycleability of LiMn2O4 cathodes by atomic layer deposition of nanosized-thin Al2O3 coatings. Nanoscale *3*, 1465.

Guilmard, M., Croguennec, L., and Delmas, C. (2003a). Thermal stability of lithium nickel oxide derivatives. Part II: $Li_xNi_{0.70}Co_{0.15}Al_{0.15}O_2$ and $Li_xNi_{0.90}Mn_{0.10}O_2$ (x = 0.50 and 0.30). Chem. Mater. *15*, 4484–4493.

Guilmard, M., Croguennec, L., Denux, D., and Delmas, C. (2003b). Thermal stability of lithium nickel oxide derivatives. Part I: Li x *Ni* 1.02 O 2 and Li x *N*i 0.89 Al 0.16 O 2 (x = *0*.50 and 0.30). Chem. Mater. *15*, 4476–4483.

Guilmard, M., Rougier, A., Grüne, M., Croguennec, L., and Delmas, C. (2003c). Effects of aluminum on the structural and electrochemical properties of LiNiO2. J. Power Sources *115*, 305–314.

Gulley, A.L., McCullough, E.A., and Shedd, K.B. (2019). China's domestic and foreign influence in the global cobalt supply chain. Resour. Policy *62*, 317–323.

International Energy Agency (2019). Global EV Outlook 2019: Scaling-Up the Transition to Electric Mobility.

Jugović, D., and Uskoković, D. (2009). A review of recent developments in the synthesis procedures of lithium iron phosphate powders. J. Power Sources *190*, 538–544.

Kan, W.H., Deng, B., Xu, Y., Shukla, A.K., Bo, T., Zhang, S., Liu, J., Pianetta, P., Wang, B.T., Liu, Y., and Chen, G. (2018). Understanding the effect of local short-range ordering on lithium diffusion in Li 1.3 Nb 0.3 Mn 0.4 O 2 single-crystal cathode. Chem *4*, 2108–2123.

Kang, W., Deng, N., Ju, J., Li, Q., Wu, D., Ma, X., Li, L., Naebe, M., and Cheng, B. (2016). A review of recent developments in rechargeable lithium–sulfur batteries. Nanoscale *8*, 16541–16588.

Kim, K.J., and Lee, J.H. (2007). Effects of nickel doping on structural and optical properties of spinel lithium manganate thin films. Solid State Commun. *141*, 99–103.

Kim, Y. (2012). Lithium nickel cobalt manganese oxide synthesized using alkali chloride flux: morphology and performance as a cathode material for lithium ion batteries. ACS Appl. Mater. Interfaces *4*, 2329–2333.

Lee, J., Urban, A., Li, X., Su, D., Hautier, G., and Ceder, G. (2014). Unlocking the potential of cation-disordered oxides for rechargeable lithium batteries. Science *343*, 519–522.

Lee, J., Papp, J.K., Clément, R.J., Sallis, S., Kwon, D.H., Shi, T., Yang, W., McCloskey, B.D., and Ceder, G. (2017). Mitigating oxygen loss to improve the cycling performance of high capacity cation-disordered cathode materials. Nat. Commun. *8*, 981.

Lee, J., Kitchaev, D.A., Kwon, D.H., Lee, C.W., Papp, J.K., Liu, Y.S., Lun, Z., Clément, R.J., Shi, T., McCloskey, B.D., et al. (2018). Reversible Mn2+/Mn4+ double redox in lithium-excess cathode materials. Nature *556*, 185–190.

Li, X., Xu, Y., and Wang, C. (2009). Suppression of Jahn–Teller distortion of spinel LiMn2O4 cathode. J. Alloys Compd. *479*, 310–313.

Li, G.R., Feng, X., Ding, Y., Ye, S.H., and Gao, X.P. (2012). AlF 3-coated Li(Li 0.17Ni 0.25Mn 0.58)O 2 as cathode material for Li-ion batteries. Electrochim. Acta *78*, 308–315.

Li, J., Downie, L.E., Ma, L., Qiu, W., and Dahn, J.R. (2015). Study of the failure mechanisms of LiNi 0.8 Mn 0.1 Co 0.1 O 2 cathode material for lithium ion batteries. J. Electrochem. Soc. *162*, A1401–A1408.

Li, Y., Bai, Y., Bi, X., Qian, J., Ma, L., Tian, J., Wu, C., Wu, F., Lu, J., and Amine, K. (2016a). An effectively activated hierarchical nano-/microspherical Li1.2Ni0.2Mn0.6O2 cathode for long-life and high-rate lithium-ion batteries. ChemSusChem *9*, 728–735.

Li, Y., Wu, C., Bai, Y., Liu, L., Wang, H., Wu, F., Zhang, N., and Zou, Y. (2016b). Hierarchical mesoporous lithium-rich Li[Li0.2Ni0.2Mn0.6]O2 cathode material synthesized via ice templating for lithium-ion battery. ACS Appl. Mater. Interfaces *8*, 18832–18840.

Li, J., Cameron, A.R., Li, H., Glazier, S., Xiong, D., Chatzidakis, M., Allen, J., Botton, G.A., and Dahn, J.R. (2017). Comparison of single crystal and polycrystalline LiNi 0.5 Mn 0.3 Co 0.2 O 2 positive electrode materials for high voltage Li-ion cells. J. Electrochem. Soc. *164*, A1534–A1544.

Li, H., Zhang, N., Li, J., and Dahn, J.R. (2018a). Updating the structure and electrochemistry of LixNiO2 for 0 ≤ x ≤ 1. J. Electrochem. Soc. *165*, A2985–A2993.

Li, M., Lu, J., Chen, Z., and Amine, K. (2018b). 30 Years of lithium-ion batteries. Adv. Mater. *30*, 1800561.

Li, H., Cormier, M., Zhang, N., Inglis, J., Li, J., and Dahn, J.R. (2019a). Is cobalt needed in Ni-rich positive electrode materials for lithium ion batteries? J. Electrochem. Soc. *166*, A429–A439.

Li, W., Asl, H.Y., Xie, Q., and Manthiram, A. (2019b). Collapse of LiNi1- x- yCoxMnyO2 lattice at deep charge irrespective of nickel content in lithium-ion batteries. J. Am. Chem. Soc. *141*, 5097–5101.

Luo, K., Roberts, M.R., Hao, R., Guerrini, N., Pickup, D.M., Liu, Y.S., Edström, K., Guo, J., Chadwick, A.V., Duda, L.C., and Bruce, P.G. (2016). Charge-compensation in 3d-transition-metal-oxide intercalation cathodes through the generation of localized electron holes on oxygen. Nat. Chem. *8*, 684–691.

Ma, S., Jiang, M., Tao, P., Song, C., Wu, J., Wang, J., Deng, T., and Shang, W. (2018). Temperature effect and thermal impact in lithium-ion batteries: a review. Prog. Nat. Sci. Mater. Int. *28*, 653–666.

Makimura, Y., Zheng, S., Ikuhara, Y., and Ukyo, Y. (2012). Microstructural observation of LiNi 0.8 Co 0.15 Al 0.05 O 2 after charge and discharge by scanning transmission electron microscopy. J. Electrochem. Soc. *159*, A1070–A1073.

Mohan, P., and Kalaignan, G.P. (2013). Structure and electrochemical performance of LiFexNi 1-xO2 (0.00 ≤ x ≤ 0.20) cathode materials for rechargeable lithium-ion batteries. J. Electroceramics *31*, 210–217.

Myung, S.T., Maglia, F., Park, K.J., Yoon, C.S., Lamp, P., Kim, S.J., and Sun, Y.K. (2017). Nickel-rich layered cathode materials for automotive lithium-ion batteries: achievements and perspectives. ACS Energ. Lett. *2*, 196–223.

Narins, T.P. (2017). The battery business: lithium availability and the growth of the global electric car industry. Extr. Ind. Soc. *4*, 321–328.

Noh, H.J., Youn, S., Yoon, C.S., and Sun, Y.K. (2013). Comparison of the structural and electrochemical properties of layered Li [NixCoyMnz]O2 (x = 1/3, 0.5, 0.6, 0.7, 0.8 and 0.85) cathode material for lithium-ion batteries. J. Power Sources *233*, 121–130.

Nykvist, B., and Nilsson, M. (2015). Rapidly falling costs of battery packs for electric vehicles. Nat. Clim. Chang. *5*, 329–332.

Olivetti, E.A., Ceder, G., Gaustad, G.G., and Fu, X. (2017). Lithium-ion battery supply chain considerations: analysis of potential bottlenecks in critical metals. Joule *1*, 229–243.

Or, T., Gourley, S.W.D., Karthikeyan, K., Yu, A., and Chen, Z. (2020). Recycling of mixed cathode lithium - ion batteries for electric vehicles: current status and future outlook. Carbon Energy *2*, 6–43.

Overland, I. (2019). The geopolitics of renewable energy: debunking four emerging myths. Energy Res. Soc. Sci. *49*, 36–40.

Pan, H., Zhang, S., Chen, J., Gao, M., Liu, Y., Zhu, T., and Jiang, Y. (2018). Li- and Mn-rich layered oxide cathode materials for lithium-ion batteries: a review from fundamentals to research progress and applications. Mol. Syst. Des. Eng. *3*, 748–803.

Schulz, K., Seal, R., Bradley, D., and Deyoung, J. (2017). Critical mineral resources of the United States—economic and environmental geology and prospects for future supply (U.S. Geological Survey).

Shin, Y., Kan, W.H., Aykol, M., Papp, J.K., McCloskey, B.D., Chen, G., and Persson, K.A. (2018). Alleviating oxygen evolution from Li-excess oxide materials through theory-guided surface protection. Nat. Commun. *9*, 4–11.

Speirs, J., Contestabile, M., Houari, Y., and Gross, R. (2014). The future of lithium availability for electric vehicle batteries. Renew. Sustain. Energy Rev. *35*, 183–193.

Sun, Y.K., Myung, S.T., Park, B.C., and Amine, K. (2006). Synthesis of spherical nano- to microscale core-shell particles Li[(Ni 0.8Co 0.1Mn 0.1) 1-x(Ni 0.5Mn 0.5) x]O 2 and their applications to lithium batteries. Chem. Mater. *18*, 5159–5163.

Sun, Y.K., Myung, S.T., Park, B.C., Prakash, J., Belharouak, I., and Amine, K. (2009). High-energy cathode material for long-life and safe lithium batteries. Nat. Mater. *8*, 320–324.

Sun, Y.-K., Kim, D.-H., Yoon, C.S., Myung, S.-T., Prakash, J., and Amine, K. (2010). A novel cathode material with a concentration-gradient for high-energy and safe lithium-ion batteries. Adv. Funct. Mater. *20*, 485–491.

Sun, Y.K., Chen, Z., Noh, H.J., Lee, D.J., Jung, H.G., Ren, Y., Wang, S., Yoon, C.S., Myung, S.T., and Amine, K. (2012). Nanostructured high-energy cathode materials for advanced lithium batteries. Nat. Mater. *11*, 942–947.

Sun, H.H., Choi, W., Lee, J.K., Oh, I.H., and Jung, H.G. (2015). Control of electrochemical properties of nickel-rich layered cathode materials for lithium ion batteries by variation of the manganese to cobalt ratio. J. Power Sources *275*, 877–883.

Thackeray, M.M., David, W.I.F., Bruce, P.G., and Goodenough, J.B. (1983). Lithium insertion into manganese spinels. Mater. Res. Bull. *18*, 461–472.

Tsurukawa, N., Prakash, S., and Manhart, A. (2011). Social impacts of artisanal cobalt mining in Katanga, Democratic Republic of Congo. Öko Institut eV Inst. Appl. Ecol. Freibg. *49*, 65.

Vikström, H., Davidsson, S., and Höök, M. (2013). Lithium availability and future production outlooks. Appl. Energ. *110*, 252–266.

Wang, D., Huang, Y., Huo, Z., and Chen, L. (2013). Synthesize and electrochemical characterization of Mg-doped Li-rich layered Li[Li0.2Ni0.2Mn0.6] O2 cathode material. Electrochim. Acta *107*, 461–466.

Wang, X., Gaustad, G., Babbitt, C.W., and Richa, K. (2014). Economies of scale for future lithium-ion battery recycling infrastructure. Resour. Conserv. Recycl. *83*, 53–62.

Wang, E., Shao, C., Qiu, S., Chu, H., Zou, Y., Xiang, C., Xu, F., and Sun, L. (2017). Organic carbon gel assisted-synthesis of Li1.2Mn0.6Ni0.2O2 for a high-performance cathode material for Li-ion batteries. RSC Adv. *7*, 1561–1566.

Watanabe, S., Kinoshita, M., Hosokawa, T., Morigaki, K., and Nakura, K. (2014). Capacity fade of LiAlyNi1-x-yCoxO 2 cathode for lithium-ion batteries during accelerated calendar and cycle life tests (surface analysis of LiAlyNi1-x-yCo xO2 cathode after cycle tests in restricted depth of discharge ranges). J. Power Sources *258*, 210–217.

Weber, R., Fell, C.R., Dahn, J.R., and Hy, S. (2017). Operando X-ray diffraction study of polycrystalline and single-crystal Li x Ni 0.5 Mn 0.3 Co 0.2 O 2. J. Electrochem. Soc. *164*, A2992–A2999.

World economic forum (2019). A Vision for a Sustainable Battery Value Chain in 2030 Unlocking the Full Potential to Power Sustainable Development and Climate Change Mitigation.

Wu, F., Xue, Q., Li, L., Zhang, X., Huang, Y., Fan, E., and Chen, R. (2017). The positive role of (NH4) 3AlF6 coating on Li[Li0.2Ni0.2Mn0.6]O2 oxide as the cathode material for lithium-ion batteries. RSC Adv. *7*, 1191–1199.

Wu, F., and Yushin, G. (2017). Conversion cathodes for rechargeable lithium and lithium-ion batteries. Energy Environ. Sci. *10*, 435–459.

Xia, Y., Zheng, J., Wang, C., and Gu, M. (2018). Designing principle for Ni-rich cathode materials with high energy density for practical applications. Nano Energy *49*, 434–452.

Xu, J., Lin, F., Doeff, M.M., and Tong, W. (2017). A review of Ni-based layered oxides for rechargeable Li-ion batteries. J. Mater. Chem. A. *5*, 874–901.

Xu, X., Huo, H., Jian, J., Wang, L., Zhu, H., Xu, S., He, X., Yin, G., Du, C., and Sun, X. (2019). Radially oriented single-crystal primary nanosheets enable ultrahigh rate and cycling properties of LiNi 0.8 Co 0.1 Mn 0.1 O 2 cathode material for lithium-ion batteries. Adv. Energy Mater. *9*, 1–9.

Yabuuchi, N., Takeuchi, M., Nakayama, M., Shiiba, H., Ogawa, M., Nakayama, K., Ohta, T., Endo, D., Ozaki, T., Inamasu, T., et al. (2015). High-capacity electrode materials for rechargeable lithium batteries: Li3NbO4-based system with cation-disordered rocksalt structure. Proc. Natl. Acad. Sci. U S A *112*, 7650–7655.

Yamada, A. (1996). Lattice instability in Li(LixMn2−x)O4. J. Solid State Chem. *122*, 160–165.

Yan, P., Zheng, J., Tang, Z.K., Devaraj, A., Chen, G., Amine, K., Zhang, J.G., Liu, L.M., and Wang, C. (2019). Injection of oxygen vacancies in the bulk lattice of layered cathodes. Nat. Nanotechnol. *14*, 602–608.

Yuan, L.X., Wang, Z.H., Zhang, W.X., Hu, X.L., Chen, J.T., Huang, Y.H., and Goodenough, J.B. (2011). Development and challenges of LiFePO4 cathode material for lithium-ion batteries. Energy Environ. Sci. *4*, 269–284.

Zeng, X., and Li, J. (2015). On the sustainability of cobalt utilization in China. Resour. Conserv. Recycl. *104*, 12–18.

Zeng, X., Zhan, C., Lu, J., and Amine, K. (2018). Stabilization of a high-capacity and high-power nickel-based cathode for Li-ion batteries. Chem *4*, 690–704.

Zeng, X., Li, M., Abd El-Hady, D., Alshitari, W., Al-Bogami, A.S., Lu, J., and Amine, K. (2019). Commercialization of lithium battery technologies for electric vehicles. Adv. Energ. Mater. *9*, 1900161.

Zhang, H.Z., Qiao, Q.Q., Li, G.R., Ye, S.H., and Gao, X.P. (2012). Surface nitridation of Li-rich layered Li(Li0.17Ni 0.25Mn0.58)O2 oxide as cathode material for lithium-ion battery. J. Mater. Chem. *22*, 13104–13109.

Zhang, N., Zaker, N., Li, H., Liu, A., Inglis, J., Jing, L., Li, J., Li, Y., Botton, G.A., and Dahn, J.R. (2019). Cobalt-free nickel-rich positive electrode materials with a core-shell structure. Chem. Mater. *31*, 10150–10160.

iScience, Volume *23*

Supplemental Information

Breaking Free from Cobalt Reliance in Lithium-Ion Batteries

Storm William D. Gourley, Tyler Or, and Zhongwei Chen

Table S1. Performance comparison of cobalt-free LIB electrodes. Commercial layered cathodes included for comparison. Performance conducted at room temperature unless specified otherwise.
*Data obtained from referenced literature sources in half-cell configuration (*vs* Li/Li^+ anode) – not representative of updated industry benchmarks.

Active Material	Average Discharge Voltage (*vs* Li/Li^+)	Initial Discharge Capacity	Initial Energy Density ($Wh\ kg^{-1}$)	Cycle Stability	Ref
Layered Transition Metal Oxides					
$Li_{1.16}Ni_{0.19}Fe_{0.18}Mn_{0.46}O_2$	3.64	232 mAh g^{-1} (2 – 4.8 V *vs* Li/Li^+, 0.1 C)	~844	73% after 100 cycles at 0.1 C	(Cheng et al., 2019)
$LiNi_{0.9}Mn_{0.1}O_2$	~3.8	236 mAh g^{-1} (2.7 – 4.4V *vs* Li/Li^+, 0.1 C)	~897	88% after 100 cycles at 0.5 C	(Aishova et al., 2020)
$LiNi_{0.85}Fe_{0.15}O_2$	~3.75	191 mAh g^{-1} (3.0 – 4.5 V *vs* Li/Li^+, 0.5 C)	~716	94% after 60 cycles at 0.5 C	(Mohan and Kalaignan, 2013)
$LiNi_{0.95}Al_{0.05}O_2$	~3.8	223 mAh g^{-1}, (3 – 4.3 V *vs* Li/Li^+, 0.05 C)	~847	96% after 50 cycles at 0.05 C	(Li et al., 2019)
O2-$Li_{1.12}Mn_{0.71}Ni_{0.17}O_2$	~3.8	220 mAh g^{-1} (2 – 4.8 V *vs* Li/Li^+, 0.05 C)	~836	77% after 50 cycles at 0.05 C	(de Boisse et al., 2018)
Core-shell $LiNi_{0.83}Al_{0.17}O_2$	~3.8	230 mAh g^{-1} (3 – 4.3 V *vs* Li/Li^+, 0.05 C)	~874	93% after 55 cycles at 0.2 C	(Zhang et al., 2019)
NMC811*	~3.7	~200 mAh g^{-1}, (3 – 4.3 V *vs* Li/Li^+, 0.2 C)	~740	70% after 100 cycles at 0.5 C	(Myung et al., 2017; Noh et al., 2013)
NMC111*	~3.7	~160 mAh g^{-1}, (3 – 4.3 V *vs* Li/Li^+, 0.2 C)	~592	92% after 100 cycles at 0.5 C	(Myung et al., 2017; Noh et al., 2013)
NCA*	~3.7	~200 mAh g^{-1}, (3 – 4.3 V *vs* Li/Li^+, 0.2 C)	~740	95% after 100 cycles at 0.2 C	(Huang et al., 2017; Noh et al., 2013)
LCO*	~3.9	~140 mAh g^{-1}, (2.7 – 4.2 V *vs* Li/Li^+, 0.2 C)	~546	88% after 50 cycles at 0.2 C	(Jiang et al., 2019)
Cation-Disordered Rocksalt					
$Li_{1.25}Nb_{0.25}V_{0.5}O_2$	~2.6	~300 mAh g^{-1}, (1.5 – 4.8 V *vs* Li/Li^+, 10 mA g^{-1} at 50 °C)	770	Stable over 20 cycles at 10 mA g^{-1}	(Nakajima and Yabuuchi, 2017)
$Li_{1.25}Nb_{0.25}Mn_{0.5}O_2$	~3.2	287 mAh g^{-1}, (1.5 – 4.8 V *vs* Li/Li^+, 10 mA g^{-1} at 55 °C)	909	71% after 20 cycles at 10 mA g^{-1}	(Wang et al., 2015)
$Li_2Mn_{2/3}Nb_{1/3}O_2F$	~3.15	317 mAh g^{-1}, (1.5 – 5 V *vs* Li/Li^+, 20 mA g^{-1})	995	66% after 25 cycles at 20 mA g^{-1}	(Lee et al., 2018)

$Li_{1.3}Nb_{0.3}Mn_{0.4}O_2$	3.1	~275 mAh g^{-1}, (1.5 – 4.8 V *vs* Li/Li^+, 10 mA g^{-1})	~853	27% after 50 cycles at 10 mA g^{-1}	(Chen et al., 2019)
Conversion					
S/Li_2S	~2.1 V	700 – 1200 mAh g^{-1} (typically 1.5 – 3 V *vs* Li/Li^+)	1500 – 2500	80% after 100 – 500 cycles	(Pope and Aksay, 2015; Wu and Yushin, 2017)

Table S2. Metal commodity prices used in cathode cost calculations in Figure 5. Accessed June 2020.

Metal	Commodity Price (USD/kg)
Al	1.57
Co	33
F (NaF)	0.5
Fe	0.16
Li (Li_2CO_3)	6
Mn	0.022
Nb (Nb_2O_5)	30.2
Ni	12.7
S	0.1
V (V_2O_5)	14.8

References

Aishova, A., Park, G.T., Yoon, C.S., Sun, Y.K., 2020. Cobalt-Free High-Capacity Ni-Rich Layered Li[Ni0.9Mn0.1]O2 Cathode. Adv. Energy Mater. 10, 1–9.

Chen, D., Kan, W.H., Chen, G., 2019. Understanding Performance Degradation in Cation-Disordered Rock-Salt Oxide Cathodes. Adv. Energy Mater. 9, 1901255.

Cheng, X., Wei, H., Hao, W., Li, H., Si, H., An, S., Zhu, W., Jia, G., Qiu, X., 2019. A Cobalt-Free Li(Li 0.16 Ni 0.19 Fe 0.18 Mn 0.46)O 2 Cathode for Lithium-Ion Batteries with Anionic Redox Reactions. ChemSusChem 12, 1162–1168.

de Boisse, B.M., Jang, J., Okubo, M., Yamada, A., 2018. Cobalt-Free O2-Type Lithium-Rich Layered Oxides. J. Electrochem. Soc. 165, A3630–A3633.

Huang, Yaqun, Huang, Yunhui, Hu, X., 2017. Enhanced electrochemical performance of LiNi0.8Co0.15Al0.05O2 by nanoscale surface modification with Co3O4. Electrochim. Acta 231, 294–299.

Jiang, Y., Qin, C., Yan, P., Sui, M., 2019. Origins of capacity and voltage fading of LiCoO2 upon high voltage cycling. J. Mater. Chem. A 7, 20824–20831.

Lee, J., Kitchaev, D.A., Kwon, D.H., Lee, C.W., Papp, J.K., Liu, Y.S., Lun, Z., Clément, R.J., Shi, T., McCloskey, B.D., Guo, J., Balasubramanian, M., Ceder, G., 2018. Reversible Mn2+/Mn4+ double redox in lithium-excess cathode materials. Nature 556, 185–190.

Li, H., Cormier, M., Zhang, N., Inglis, J., Li, J., Dahn, J.R., 2019. Is cobalt needed in Ni-rich positive electrode materials for lithium ion batteries? J. Electrochem. Soc. 166, A429–A439.

Mohan, P., Kalaignan, G.P., 2013. Structure and electrochemical performance of LiFexNi 1-xO2 ($0.00 \leq x \leq 0.20$) cathode materials for rechargeable lithium-ion batteries. J. Electroceramics 31, 210–217.

Myung, S.T., Maglia, F., Park, K.J., Yoon, C.S., Lamp, P., Kim, S.J., Sun, Y.K., 2017. Nickel-Rich Layered Cathode Materials for Automotive Lithium-Ion Batteries: Achievements and Perspectives. ACS Energy Lett.

Nakajima, M., Yabuuchi, N., 2017. Lithium-Excess Cation-Disordered Rocksalt-Type Oxide with Nanoscale Phase Segregation: Li1.25Nb0.25V0.5O2. Chem. Mater. 29, 6927–6935.

Noh, H.J., Youn, S., Yoon, C.S., Sun, Y.K., 2013. Comparison of the structural and electrochemical properties of layered Li[NixCoyMnz]O2 (x = 1/3, 0.5, 0.6, 0.7, 0.8 and 0.85) cathode material for lithium-ion batteries. J. Power Sources 233, 121–130.

Pope, M.A., Aksay, I.A., 2015. Structural Design of Cathodes for Li-S Batteries. Adv. Energy Mater. 5, 1500124.

Wang, R., Li, X., Liu, L., Lee, J., Seo, D.H., Bo, S.H., Urban, A., Ceder, G., 2015. A disordered rock-salt Li-excess cathode material with high capacity and substantial oxygen redox activity: Li1.25Nb0.25Mn0.5O2. Electrochem. commun. 60, 70–73.

Wu, F., Yushin, G., 2017. Conversion cathodes for rechargeable lithium and lithium-ion batteries. Energy Environ. Sci.

Zhang, N., Zaker, N., Li, H., Liu, A., Inglis, J., Jing, L., Li, J., Li, Y., Botton, G.A., Dahn, J.R., 2019. Cobalt-Free Nickel-Rich Positive Electrode Materials with a Core-Shell Structure. Chem. Mater. 31, 10150–10160.